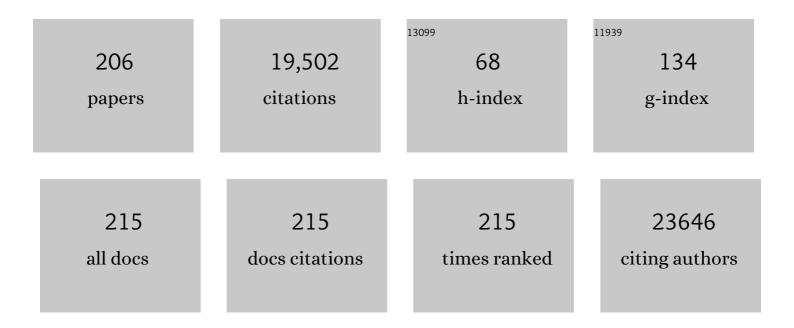
## Bo Chen

## List of Publications by Year in descending order

Source: https://exaly.com/author-pdf/834503/publications.pdf Version: 2024-02-01



RO CHEN

#	Article	IF	CITATIONS
1	The anatomical, electrophysiological and histological observations of muscle contraction units in rabbits: a new perspective on nerve injury and regeneration. Neural Regeneration Research, 2022, 17, 228.	3.0	1
2	Synthesis of Pd <sub>3</sub> Sn and PdCuSn Nanorods with <i>L1<sub>2</sub></i> Phase for Highly Efficient Electrocatalytic Ethanol Oxidation. Advanced Materials, 2022, 34, e2106115.	21.0	65
3	Preparation of <i>fcc</i> â€2Hâ€ <i>fcc</i> Heterophase Pd@lr Nanostructures for Highâ€Performance Electrochemical Hydrogen Evolution. Advanced Materials, 2022, 34, e2107399.	21.0	48
4	Two-dimensional covalent organic framework nanosheets: Synthesis and energy-related applications. Chinese Chemical Letters, 2022, 33, 2867-2882.	9.0	17
5	Rapid semi-quantitative analysis of hemolytic triterpenoid saponins in Lonicerae Flos crude drugs and preparations by paper spray mass spectrometry. Talanta, 2022, 239, 123148.	5.5	4
6	Parametric design approach on high-order and multi-segment modified elliptical helical gears based on virtual gear shaping. Proceedings of the Institution of Mechanical Engineers, Part C: Journal of Mechanical Engineering Science, 2022, 236, 4599-4609.	2.1	4
7	Bimetallic Bi–Sn microspheres as high initial coulombic efficiency and long lifespan anodes for sodium-ion batteries. Chemical Communications, 2022, 58, 5140-5143.	4.1	15
8	Intercalation of organics into layered structures enables superior interface compatibility and fast charge diffusion for dendrite-free Zn anodes. Energy and Environmental Science, 2022, 15, 1682-1693.	30.8	105
9	Mesocarbon Microbeads Boost the Electrochemical Performances of LiFePO <sub>4</sub>   Li <sub>4</sub> Ti <sub>5</sub> O <sub>12</sub> through Anion Intercalation. ChemSusChem, 2022, 15, .	6.8	7
10	Isoreticular Series of Two-Dimensional Covalent Organic Frameworks with the kgd Topology and Controllable Micropores. Journal of the American Chemical Society, 2022, 144, 6475-6482.	13.7	41
11	Confined Growth of Silver–Copper Janus Nanostructures with {100} Facets for Highly Selective Tandem Electrocatalytic Carbon Dioxide Reduction. Advanced Materials, 2022, 34, e2110607.	21.0	82
12	Preparation of Au@Pd Core–Shell Nanorods with <i>fcc</i> -2H- <i>fcc</i> Heterophase for Highly Efficient Electrocatalytic Alcohol Oxidation. Journal of the American Chemical Society, 2022, 144, 547-555.	13.7	88
13	Hybridization of 2D Nanomaterials with 3D Graphene Architectures for Electrochemical Energy Storage and Conversion. Advanced Functional Materials, 2022, 32, .	14.9	26
14	Land Subsidence in Qingdao, China, from 2017 to 2020 Based on PS-InSAR. International Journal of Environmental Research and Public Health, 2022, 19, 4913.	2.6	5
15	Saltâ€Assisted 2Hâ€ŧoâ€1T′ Phase Transformation of Transition Metal Dichalcogenides. Advanced Materials, 2022, 34, e2201194.	21.0	19
16	Preparation of Amorphous SnO <sub>2</sub> â€Encapsulated Multiphased Crystalline Cu Heterostructures for Highly Efficient CO <sub>2</sub> Reduction. Advanced Materials, 2022, 34, e2201114.	21.0	29
17	Decreasing the Overpotential of Aprotic Li O <sub>2</sub> Batteries with the Inâ€Plane Alloy Structure in Ultrathin 2D Ruâ€Based Nanosheets. Advanced Functional Materials, 2022, 32, .	14.9	39
18	Analysis of the Longitudinal-Bending-Torsional Coupled Vibration Mechanism of the Drilling of a Roof Bolter for Mine Support System. Mathematical Problems in Engineering, 2022, 2022, 1-14.	1.1	0

#	Article	IF	CITATIONS
19	Ruthenium nanoclusters anchored on cobalt phosphide hollow microspheres by green phosphating process for full water splitting in acidic electrolyte. Chinese Chemical Letters, 2021, 32, 511-515.	9.0	46
20	Liquid Nanoparticles: Manipulating the Nucleation and Growth of Nanoscale Droplets. Angewandte Chemie - International Edition, 2021, 60, 3047-3054.	13.8	18
21	Liquid Nanoparticles: Manipulating the Nucleation and Growth of Nanoscale Droplets. Angewandte Chemie, 2021, 133, 3084-3091.	2.0	4
22	Quasiâ€Epitaxial Growth of Magnetic Nanostructures on 4Hâ€Au Nanoribbons. Advanced Materials, 2021, 33, e2007140.	21.0	18
23	Ultrathin Amorphous/Crystalline Heterophase Rh and Rh Alloy Nanosheets as Tandem Catalysts for Direct Indole Synthesis. Advanced Materials, 2021, 33, e2006711.	21.0	68
24	Bifunctional single-molecular heterojunction enables completely selective CO <sub>2</sub> -to-CO conversion integrated with oxidative 3D nano-polymerization. Energy and Environmental Science, 2021, 14, 1544-1552.	30.8	95
25	A solvent decomposition and explosion approach for boron nanoplate synthesis. Chemical Communications, 2021, 57, 4922-4925.	4.1	3
26	Research on the Dynamic Path Planning of Manipulators Based on a Grid-Local Probability Road Map Method. IEEE Access, 2021, 9, 101186-101196.	4.2	5
27	Silicate-Enhanced Heterogeneous Flow-Through Electro-Fenton System Using Iron Oxides under Nanoconfinement. Environmental Science & Technology, 2021, 55, 4045-4053.	10.0	192
28	Rücktitelbild: Liquid Nanoparticles: Manipulating the Nucleation and Growth of Nanoscale Droplets (Angew. Chem. 6/2021). Angewandte Chemie, 2021, 133, 3352-3352.	2.0	0
29	Preparation of CdS <i><sub>y</sub></i> Se <sub>1â^'</sub> <i><sub>y</sub></i> â€MoS <sub>2</sub> Heterostructures via Cation Exchange of Preâ€Epitaxially Synthesized Cu <sub>2â^'</sub> <i><sub>i‡</sub></i> S <i><sub>y</sub></i> Se <sub>1â^'</sub> <i><sub>y</sub></i> for Photocatalytic Hydrogen Evolution. Small, 2021, 17, e2006135.	<sub>2<td>sub&gt;</td></sub>	sub>
30	Investigation into surface composition of nitrogen-doped niobium for superconducting RF cavities. Nanotechnology, 2021, 32, 245701.	2.6	4
31	Selective Epitaxial Growth of Rh Nanorods on 2H/ <i>fcc</i> Heterophase Au Nanosheets to Form 1D/2D Rh–Au Heterostructures for Highly Efficient Hydrogen Evolution. Journal of the American Chemical Society, 2021, 143, 4387-4396.	13.7	56
32	Evoking ordered vacancies in metallic nanostructures toward a vacated Barlow packing for high-performance hydrogen evolution. Science Advances, 2021, 7, .	10.3	64
33	High‥ield Exfoliation of Ultrathin 2D Ni <sub>3</sub> Cr <sub>2</sub> P <sub>2</sub> S <sub>9</sub> and Ni <sub>3</sub> Cr <sub>2</sub> P <sub>2</sub> Se <sub>9</sub> Nanosheets. Small, 2021, 17, e2006866.	10.0	8
34	A Gasâ€Phase Migration Strategy to Synthesize Atomically Dispersed Mnâ€N  Catalysts for Zn–Air Batteries. Small Methods, 2021, 5, e2100024.	8.6	44
35	Metastable 1T′-phase group VIB transition metal dichalcogenide crystals. Nature Materials, 2021, 20, 1113-1120.	27.5	119
36	Suppressing the intestinal farnesoid X receptor/sphingomyelin phosphodiesterase 3 axis decreases atherosclerosis. Journal of Clinical Investigation, 2021, 131, .	8.2	50

#	Article	IF	CITATIONS
37	Hydrogen-Intercalation-Induced Lattice Expansion of Pd@Pt Core–Shell Nanoparticles for Highly Efficient Electrocatalytic Alcohol Oxidation. Journal of the American Chemical Society, 2021, 143, 11262-11270.	13.7	121
38	Macrophage HIF-2α suppresses NLRP3 inflammasome activation and alleviates insulin resistance. Cell Reports, 2021, 36, 109607.	6.4	32
39	Defect-Rich Hierarchical Porous UiO-66(Zr) for Tunable Phosphate Removal. Environmental Science & Technology, 2021, 55, 13209-13218.	10.0	27
40	Glutathione-mediated formation of disulfide bonds modulates the properties of myofibrillar protein gels at different temperatures. Food Chemistry, 2021, 364, 130356.	8.2	29
41	Tipâ€Enhanced Electric Field: A New Mechanism Promoting Mass Transfer in Oxygen Evolution Reactions. Advanced Materials, 2021, 33, e2007377.	21.0	179
42	Seeded Synthesis of Unconventional 2H-Phase Pd Alloy Nanomaterials for Highly Efficient Oxygen Reduction. Journal of the American Chemical Society, 2021, 143, 17292-17299.	13.7	59
43	Microfluidic Chip-Based Induced Phase Separation Extraction as a Fast and Efficient Miniaturized Sample Preparation Method. Molecules, 2021, 26, 38.	3.8	8
44	Layered Transition Metal Dichalcogenideâ€Based Nanomaterials for Electrochemical Energy Storage. Advanced Materials, 2020, 32, e1903826.	21.0	329
45	Rapid microwaveâ€assisted Porter method for determination of proanthocyanidins. Phytochemical Analysis, 2020, 31, 215-220.	2.4	1
46	Stochastic micromechanical predictions for the probabilistic behavior of saturated concrete repaired by the electrochemical deposition method. International Journal of Damage Mechanics, 2020, 29, 435-453.	4.2	18
47	Synthesis of a poly(sulfobetaine-co-polyhedral oligomeric silsesquioxane) hybrid monolith via an in-situ ring opening quaternization for use in hydrophilic interaction capillary liquid chromatography. Mikrochimica Acta, 2020, 187, 109.	5.0	8
48	An assessment of melamine exposure in Shanghai adults and its association with food consumption. Environment International, 2020, 135, 105363.	10.0	27
49	Phase-Selective Epitaxial Growth of Heterophase Nanostructures on Unconventional 2H-Pd Nanoparticles. Journal of the American Chemical Society, 2020, 142, 18971-18980.	13.7	111
50	Molten Salt-Directed Catalytic Synthesis of 2D Layered Transition-Metal Nitrides for Efficient Hydrogen Evolution. CheM, 2020, 6, 2382-2394.	11.7	163
51	Intensive Versus Extensive Events? Insights from Cumulative Flood-Induced Mortality Over the Globe, 1976–2016. International Journal of Disaster Risk Science, 2020, 11, 441-451.	2.9	17
52	Development of Biomimetic Synthesis of Propindilactone G <sup>â€</sup> . Chinese Journal of Chemistry, 2020, 38, 1339-1352.	4.9	7
53	Precise Dimerization of Hollow Fullerene Compartments. Journal of the American Chemical Society, 2020, 142, 15396-15402.	13.7	22
54	A universal method for rapid and largeâ€scale growth of layered crystals. SmartMat, 2020, 1, e1011.	10.7	33

#	Article	IF	CITATIONS
55	Crystal phase-controlled growth of PtCu and PtCo alloys on 4H Au nanoribbons for electrocatalytic ethanol oxidation reaction. Nano Research, 2020, 13, 1970-1975.	10.4	32
56	Covalency competition dominates the water oxidation structure–activity relationship on spinel oxides. Nature Catalysis, 2020, 3, 554-563.	34.4	284
57	Ethylene Selectivity in Electrocatalytic CO <sub>2</sub> Reduction on Cu Nanomaterials: A Crystal Phase-Dependent Study. Journal of the American Chemical Society, 2020, 142, 12760-12766.	13.7	183
58	Optical Spectroscopy of Single Colloidal CsPbBr <sub>3</sub> Perovskite Nanoplatelets. Nano Letters, 2020, 20, 3673-3680.	9.1	47
59	Transition metal dichalcogenide/multi-walled carbon nanotube-based fibers as flexible electrodes for electrocatalytic hydrogen evolution. Chemical Communications, 2020, 56, 5131-5134.	4.1	28
60	Heterophase fcc-2H-fcc gold nanorods. Nature Communications, 2020, 11, 3293.	12.8	92
61	Intramolecular Hydrogen Bonding-Based Topology Regulation of Two-Dimensional Covalent Organic Frameworks. Journal of the American Chemical Society, 2020, 142, 13162-13169.	13.7	85
62	Bioinspired Synthesis of Nortriterpenoid Propindilactone G. Journal of the American Chemical Society, 2020, 142, 5007-5012.	13.7	32
63	Impeding Catalyst Sulfur Poisoning in Aqueous Solution by Metal–Organic Framework Composites. Small Methods, 2020, 4, 1900890.	8.6	22
64	Metal–organic framework-derived mesoporous carbon nanoframes embedded with atomically dispersed Fe–N active sites for efficient bifunctional oxygen and carbon dioxide electroreduction. Applied Catalysis B: Environmental, 2020, 267, 118720.	20.2	151
65	Ligandâ€Exchangeâ€Induced Amorphization of Pd Nanomaterials for Highly Efficient Electrocatalytic Hydrogen Evolution Reaction. Advanced Materials, 2020, 32, e1902964.	21.0	164
66	Synthesis of Palladiumâ€Based Crystalline@Amorphous Core–Shell Nanoplates for Highly Efficient Ethanol Oxidation. Advanced Materials, 2020, 32, e2000482.	21.0	98
67	Imparting Boron Nanosheets with Ambient Stability through Methyl Group Functionalization for Mechanistic Investigation of Their Lithiation Process. ACS Applied Materials & Interfaces, 2020, 12, 23370-23377.	8.0	15
68	Selective Epitaxial Growth of Oriented Hierarchical Metal–Organic Framework Heterostructures. Journal of the American Chemical Society, 2020, 142, 8953-8961.	13.7	100
69	Bimetallic oxide coupled with B-doped graphene as highly efficient electrocatalyst for oxygen evolution reaction. Science China Materials, 2020, 63, 1247-1256.	6.3	14
70	Construction of a Sandwiched MOF@COF Composite as a Size-Selective Catalyst. Cell Reports Physical Science, 2020, 1, 100272.	5.6	21
71	The establishment of the fertile fish lineages derived from distant hybridization by overcoming the reproductive barriers. Reproduction, 2020, 159, R237-R249.	2.6	17
72	Defect-Rich, Candied Haws-Shaped AuPtNi Alloy Nanostructures for Highly Efficient Electrocatalysis. CCS Chemistry, 2020, 2, 24-30.	7.8	23

#	Article	IF	CITATIONS
73	A simple electrochemical method for conversion of Pt wires to Pt concave icosahedra and nanocubes on carbon paper for electrocatalytic hydrogen evolution. Science China Materials, 2019, 62, 115-121.	6.3	16
74	lron-facilitated dynamic active-site generation on spinel CoAl2O4 with self-termination of surface reconstruction for water oxidation. Nature Catalysis, 2019, 2, 763-772.	34.4	678
75	Effect of glutenin and gliadin modified by protein-glutaminase on retrogradation properties and digestibility of potato starch. Food Chemistry, 2019, 301, 125226.	8.2	43
76	Aging amorphous/crystalline heterophase PdCu nanosheets for catalytic reactions. National Science Review, 2019, 6, 955-961.	9.5	75
77	Unusual 4H-phase twinned noble metal nanokites. Nature Communications, 2019, 10, 2881.	12.8	25
78	Synthesis of RuNi alloy nanostructures composed of multilayered nanosheets for highly efficient electrocatalytic hydrogen evolution. Nano Energy, 2019, 66, 104173.	16.0	116
79	Heterostructured TiO <sub>2</sub> Spheres with Tunable Interiors and Shells toward Improved Packing Density and Pseudocapacitive Sodium Storage. Advanced Materials, 2019, 31, e1904589.	21.0	73
80	Elemental Segregation in Multimetallic Core–Shell Nanoplates. Journal of the American Chemical Society, 2019, 141, 14496-14500.	13.7	46
81	Sizeâ€Ðependent Phase Transformation of Noble Metal Nanomaterials. Small, 2019, 15, e1903253.	10.0	16
82	Analysis of Chromosomal Numbers, Mitochondrial Genome, and Full-Length Transcriptome of Onychostoma brevibarba. Marine Biotechnology, 2019, 21, 515-525.	2.4	5
83	Free-standing 2D nanorafts by assembly of 1D nanorods for biomolecule sensing. Nanoscale, 2019, 11, 12169-12176.	5.6	30
84	MOFâ€Based Hierarchical Structures for Solarâ€Thermal Clean Water Production. Advanced Materials, 2019, 31, e1808249.	21.0	233
85	Progressively Exposing Active Facets of 2D Nanosheets toward Enhanced Pseudocapacitive Response and Highâ€Rate Sodium Storage. Advanced Materials, 2019, 31, e1900526.	21.0	83
86	Rapid quantitative analysis of ginkgo flavonoids using paper spray mass spectrometry. Journal of Pharmaceutical and Biomedical Analysis, 2019, 171, 158-163.	2.8	12
87	Spatial Variability and Temporal Persistence of Event Runoff Coefficients for Cropland Hillslopes. Water Resources Research, 2019, 55, 1583-1597.	4.2	21
88	N- and S- co-doped graphene sheet-encapsulated Co9S8 nanomaterials as excellent electrocatalysts for the oxygen evolution reaction. Journal of Power Sources, 2019, 417, 90-98.	7.8	52
89	Synthesis of PdM (M = Zn, Cd, ZnCd) Nanosheets with an Unconventional Face-Centered Tetragonal Phase as Highly Efficient Electrocatalysts for Ethanol Oxidation. ACS Nano, 2019, 13, 14329-14336.	14.6	133
90	The fabrication of poly (polyethylene glycol diacrylate) monolithic porous layer open tubular (monoâ€PLOT) columns and applications in hydrophilic interaction chromatography and capillary gas chromatography for small molecules. Electrophoresis, 2019, 40, 521-529.	2.4	7

#	Article	IF	CITATIONS
91	Pulsed elution modulation for on-line comprehensive two-dimensional liquid chromatography coupling reversed phase liquid chromatography and hydrophilic interaction chromatography. Journal of Chromatography A, 2019, 1583, 98-107.	3.7	21
92	Synthesis of MoX2 (X = Se or S) monolayers with high-concentration 1T′ phase on 4H/fcc-Au nanorods for hydrogen evolution. Nano Research, 2019, 12, 1301-1305.	10.4	44
93	A Special Issue on Advanced Hybrid Nanomaterials for Energy Conversion and Storage. Science of Advanced Materials, 2019, 11, 307-310.	0.7	3
94	Water transport confined in graphene oxide channels through the rarefied effect. Physical Chemistry Chemical Physics, 2018, 20, 9780-9786.	2.8	23
95	Transformable masks for colloidal nanosynthesis. Nature Communications, 2018, 9, 563.	12.8	67
96	Natural meroterpenoids isolated from the plant pathogenic fungus Verticillium albo-atrum with noteworthy modification action against voltage-gated sodium channels of central neurons of Helicoverpa armigera. Pesticide Biochemistry and Physiology, 2018, 144, 91-99.	3.6	8
97	Construction of 4â€lsochromanones through Cu(OTf) <sub>2</sub> â€Catalysed Sequential C=O and C–O Bond Formation. European Journal of Organic Chemistry, 2018, 2018, 926-931.	2.4	9
98	Transforming Monolayer Transition-Metal Dichalcogenide Nanosheets into One-Dimensional Nanoscrolls with High Photosensitivity. ACS Applied Materials & Interfaces, 2018, 10, 13011-13018.	8.0	45
99	Hybridization of MOFs and COFs: A New Strategy for Construction of MOF@COF Core–Shell Hybrid Materials. Advanced Materials, 2018, 30, 1705454.	21.0	318
100	Gut microbiota and intestinal FXR mediate the clinical benefits of metformin. Nature Medicine, 2018, 24, 1919-1929.	30.7	632
101	Realization of vertical metal semiconductor heterostructures via solution phase epitaxy. Nature Communications, 2018, 9, 3611.	12.8	49
102	Controllable Design of MoS <sub>2</sub> Nanosheets Anchored on Nitrogenâ€Doped Graphene: Toward Fast Sodium Storage by Tunable Pseudocapacitance. Advanced Materials, 2018, 30, e1800658.	21.0	275
103	Rapid Analysis of Illegal Cationic Dyes in Foods and Surface Waters Using High Temperature Direct Analysis in Real Time High-Resolution Mass Spectrometry. Journal of Agricultural and Food Chemistry, 2018, 66, 7542-7549.	5.2	23
104	Enlarged CoO Covalency in Octahedral Sites Leading to Highly Efficient Spinel Oxides for Oxygen Evolution Reaction. Advanced Materials, 2018, 30, e1802912.	21.0	338
105	Rapid analysis of benzoic acid and vitamin C in beverages by paper spray mass spectrometry. Food Chemistry, 2018, 268, 411-415.	8.2	29
106	Synthesis of Hierarchical 4H/fcc Ru Nanotubes for Highly Efficient Hydrogen Evolution in Alkaline Media. Small, 2018, 14, e1801090.	10.0	80
107	A River Channel Extraction Method for Urban Environments Based on Terrain Transition Lines. Water Resources Research, 2018, 54, 4887-4900.	4.2	4
108	Two-Dimensional Metal Nanomaterials: Synthesis, Properties, and Applications. Chemical Reviews, 2018, 118, 6409-6455.	47.7	711

#	Article	IF	CITATIONS
109	Amorphous/Crystalline Heteroâ€Phase Pd Nanosheets: Oneâ€Pot Synthesis and Highly Selective Hydrogenation Reaction. Advanced Materials, 2018, 30, e1803234.	21.0	231
110	Preparation of 1Tâ€2-Phase ReS <sub>2<i>x</i></sub> Se <sub>2(1-<i>x</i>)</sub> ( <i>x</i> = 0–1) Nanodots for Highly Efficient Electrocatalytic Hydrogen Evolution Reaction. Journal of the American Chemical Society, 2018, 140, 8563-8568.	13.7	104
111	Crystal Phase and Architecture Engineering of Lotusâ€Thalamusâ€Shaped Ptâ€Ni Anisotropic Superstructures for Highly Efficient Electrochemical Hydrogen Evolution. Advanced Materials, 2018, 30, e1801741.	21.0	163
112	Flood-induced mortality across the globe: Spatiotemporal pattern and influencing factors. Science of the Total Environment, 2018, 643, 171-182.	8.0	156
113	Improved Reversibility of Fe <sup>3+</sup> /Fe <sup>4+</sup> Redox Couple in Sodium Super Ion Conductor Type Na <sub>3</sub> Fe <sub>2</sub> (PO <sub>4</sub> ) <sub>3</sub> for Sodiumâ€lon Batteries. Advanced Materials, 2017, 29, 1605694.	21.0	169
114	Rapid analysis of Aurantii Fructus Immaturus (Zhishi) using paper spray ionization mass spectrometry. Journal of Pharmaceutical and Biomedical Analysis, 2017, 137, 204-212.	2.8	18
115	New urea-modified paper substrate for enhanced analytical performance of negative ion mode paper spray mass spectrometry. Talanta, 2017, 166, 306-314.	5.5	31
116	General Fabrication of Boride, Carbide, and Nitride Nanocrystals via a Metal-Hydrolysis-Assisted Process. Inorganic Chemistry, 2017, 56, 2440-2447.	4.0	23
117	Rapid Analysis of <i>Corni fructus</i> Using Paper Sprayâ€Mass Spectrometry. Phytochemical Analysis, 2017, 28, 344-350.	2.4	14
118	Polymerization of polyhedral oligomeric silsequioxane (POSS) with perfluoro-monomers and a kinetic study. RSC Advances, 2017, 7, 10700-10706.	3.6	5
119	Preparation of Ultrathin Twoâ€Dimensional Ti <sub><i>x</i></sub> Ta <sub>1â^'<i>x</i></sub> S <sub><i>y</i></sub> O <sub><i>z</i></sub> Nanosheets as Highly Efficient Photothermal Agents. Angewandte Chemie - International Edition, 2017, 56, 7842-7846.	13.8	59
120	Preparation of Ultrathin Twoâ€Dimensional Ti <sub><i>x</i></sub> Ta <sub>1â^'<i>x</i></sub> S <sub><i>y</i></sub> O <sub><i>z</i></sub> Nanosheets as Highly Efficient Photothermal Agents. Angewandte Chemie, 2017, 129, 7950-7954.	2.0	11
121	Anodized Aluminum Oxide Templated Synthesis of Metal–Organic Frameworks Used as Membrane Reactors. Angewandte Chemie - International Edition, 2017, 56, 578-581.	13.8	57
122	Interdiffusion Reaction-Assisted Hybridization of Two-Dimensional Metal–Organic Frameworks and Ti <sub>3</sub> C <sub>2</sub> T <sub><i>x</i></sub> Nanosheets for Electrocatalytic Oxygen Evolution. ACS Nano, 2017, 11, 5800-5807.	14.6	557
123	Growth of Au Nanoparticles on 2D Metalloporphyrinic Metalâ€Organic Framework Nanosheets Used as Biomimetic Catalysts for Cascade Reactions. Advanced Materials, 2017, 29, 1700102.	21.0	384
124	The synthesis of Gemini-type sulfobetaine based hybrid monolith and its application in hydrophilic interaction chromatography for small polar molecular. Talanta, 2017, 173, 113-122.	5.5	9
125	Rapid Analysis of Bisphenol A and Its Analogues in Food Packaging Products by Paper Spray Ionization Mass Spectrometry. Journal of Agricultural and Food Chemistry, 2017, 65, 4859-4865.	5.2	38
126	Ultrathin Two-Dimensional Covalent Organic Framework Nanosheets: Preparation and Application in Highly Sensitive and Selective DNA Detection. Journal of the American Chemical Society, 2017, 139, 8698-8704.	13.7	440

#	Article	IF	CITATIONS
127	Composition- and phase-controlled synthesis and applications of alloyed phase heterostructures of transition metal disulphides. Nanoscale, 2017, 9, 5102-5109.	5.6	63
128	Ultrathin Twoâ€Dimensional Organic–Inorganic Hybrid Perovskite Nanosheets with Bright, Tunable Photoluminescence and High Stability. Angewandte Chemie - International Edition, 2017, 56, 4252-4255.	13.8	206
129	Anodized Aluminum Oxide Templated Synthesis of Metal–Organic Frameworks Used as Membrane Reactors. Angewandte Chemie, 2017, 129, 593-596.	2.0	18
130	The colour combination method for human-machine interfaces driven by colour images. Journal of Engineering Design, 2017, 28, 505-531.	2.3	5
131	Orthogonal strategy development using reversed macroporous resin coupled with hydrophilic interaction liquid chromatography for the separation of ginsenosides from ginseng root extract. Journal of Separation Science, 2017, 40, 4128-4134.	2.5	8
132	The preparation of a poly (pentaerythritol tetraglycidyl ether-co-poly ethylene imine) organic monolithic capillary column and its application in hydrophilic interaction chromatography for polar molecules. Analytica Chimica Acta, 2017, 988, 104-113.	5.4	12
133	Synthesis of WO <sub><i>n</i></sub> â€WX <sub>2</sub> ( <i>n</i> =2.7, 2.9; X=S, Se) Heterostructures for Highly Efficient Green Quantum Dot Lightâ€Emitting Diodes. Angewandte Chemie, 2017, 129, 10622-10626.	2.0	7
134	Synthesis of WO <sub><i>n</i></sub> â€WX <sub>2</sub> ( <i>n</i> =2.7, 2.9; X=S, Se) Heterostructures for Highly Efficient Green Quantum Dot Lightâ€Emitting Diodes. Angewandte Chemie - International Edition, 2017, 56, 10486-10490.	13.8	21
135	Preparation of graphene-MoS2 hybrid aerogels as multifunctional sorbents for water remediation. Science China Materials, 2017, 60, 1102-1108.	6.3	27
136	Synthesis of Ultrathin PdCu Alloy Nanosheets Used as a Highly Efficient Electrocatalyst for Formic Acid Oxidation. Advanced Materials, 2017, 29, 1700769.	21.0	207
137	Rapid analysis of benzalkonium chloride using paper spray mass spectrometry. Journal of Pharmaceutical and Biomedical Analysis, 2017, 145, 151-157.	2.8	4
138	Association of Dietary Pattern during Pregnancy and Gestational Diabetes Mellitus: A Prospective Cohort Study in Northern China. Biomedical and Environmental Sciences, 2017, 30, 887-897.	0.2	19
139	Characteristics of aquatic bacterial community and the influencing factors in an urban river. Science of the Total Environment, 2016, 569-570, 382-389.	8.0	72
140	Weavable, Highâ€Performance, Solidâ€State Supercapacitors Based on Hybrid Fibers Made of Sandwiched Structure of MWCNT/rGO/MWCNT. Advanced Electronic Materials, 2016, 2, 1600102.	5.1	47
141	Preparation of Singleâ€Layer MoS <sub>2</sub> <i><sub>x</sub></i> Se <sub>2(1â€</sub> <i><sub>x</sub></i> <sub><sub><sub>x</sub> Mo<i><sub>x</sub></i>W<sub>1â€</sub><i><sub>x</sub></i>S<sub>2</sub> Nanosheets with Highâ€Concentration Metallic 1T Phase, Small, 2016, 12, 1866-1874.</sub></sub>	10.0	126
142	Bioinspired Design of Ultrathin 2D Bimetallic Metal–Organicâ€Framework Nanosheets Used as Biomimetic Enzymes. Advanced Materials, 2016, 28, 4149-4155.	21.0	440
143	Structure of the Upper Mantle and Transition Zone Beneath the South China Block Imaged by Finite Frequency Tomography. Acta Geologica Sinica, 2016, 90, 1637-1652.	1.4	10
144	Single Particle Tracking of Peptides-Modified Nanocargo on Lipid Membrane Revealing Bulk-Mediated Diffusion. Analytical Chemistry, 2016, 88, 11973-11977.	6.5	21

#	Article	IF	CITATIONS
145	Characterization of Oxygenates in Zhundong Subbituminous Coal by Gas Chromatography/Mass Spectrometry. Analytical Letters, 2016, 49, 1359-1365.	1.8	4
146	Fabrication of folic acid-sensitive gold nanoclusters for turn-on fluorescent imaging of overexpression of folate receptor in tumor cells. Talanta, 2016, 158, 118-124.	5.5	36
147	Synthesis of Two-Dimensional CoS <sub>1.097</sub> /Nitrogen-Doped Carbon Nanocomposites Using Metal–Organic Framework Nanosheets as Precursors for Supercapacitor Application. Journal of the American Chemical Society, 2016, 138, 6924-6927.	13.7	591
148	Facile fabrication of hydrophobic octadecylamine-functionalized polyurethane foam for oil spill cleanup. Journal of Macromolecular Science - Pure and Applied Chemistry, 2016, 53, 196-200.	2.2	9
149	Self-Assembled Fluorescent Bovine Serum Albumin Nanoprobes for Ratiometric pH Measurement inside Living Cells. ACS Applied Materials & Interfaces, 2016, 8, 9629-9634.	8.0	47
150	Oneâ€Pot Synthesis of Highly Anisotropic Fiveâ€Foldâ€Twinned PtCu Nanoframes Used as a Bifunctional Electrocatalyst for Oxygen Reduction and Methanol Oxidation. Advanced Materials, 2016, 28, 8712-8717.	21.0	336
151	Quantification of Cancer Biomarkers in Serum Using Scattering-Based Quantitative Single Particle Intensity Measurement with a Dark-Field Microscope. Analytical Chemistry, 2016, 88, 8849-8856.	6.5	81
152	A bright carbon-dot-based fluorescent probe for selective and sensitive detection of mercury ions. Talanta, 2016, 161, 476-481.	5.5	75
153	The synthesis of surface-glycosylated porous monolithic column via aqueous two-phase graft copolymerization and its application in capillary-liquid chromatography. Talanta, 2016, 161, 721-729.	5.5	7
154	In Situ Synthesis of Metal Sulfide Nanoparticles Based on 2D Metalâ€Organic Framework Nanosheets. Small, 2016, 12, 4669-4674.	10.0	101
155	Selfâ€Assembly of Singleâ€Layer CoAlâ€Layered Double Hydroxide Nanosheets on 3D Graphene Network Used as Highly Efficient Electrocatalyst for Oxygen Evolution Reaction. Advanced Materials, 2016, 28, 7640-7645.	21.0	355
156	Submonolayered Ru Deposited on Ultrathin Pd Nanosheets used for Enhanced Catalytic Applications. Advanced Materials, 2016, 28, 10282-10286.	21.0	148
157	Redistribution of fluorescent molecules at the solid/liquid interface with total internal reflection illumination. Talanta, 2016, 155, 229-234.	5.5	0
158	Facile "one-pot―synthesis of poly(methacrylic acid)-based hybrid monolith via thiol-ene click reaction for hydrophilic interaction chromatography. Journal of Chromatography A, 2016, 1454, 49-57.	3.7	21
159	MoS2-coated vertical graphene nanosheet for high-performance rechargeable lithium-ion batteries and hydrogen production. NPG Asia Materials, 2016, 8, e268-e268.	7.9	113
160	Hybrid Flexible Resistive Random Access Memoryâ€Gated Transistor for Novel Nonvolatile Data Storage. Small, 2016, 12, 390-396.	10.0	42
161	2D Transitionâ€Metalâ€Dichalcogenideâ€Nanosheetâ€Based Composites for Photocatalytic and Electrocatalytic Hydrogen Evolution Reactions. Advanced Materials, 2016, 28, 1917-1933.	21.0	1,214
162	Levelling the playing field: screening for synergistic effects in coalesced bimetallic nanoparticles. Nanoscale, 2016, 8, 3447-3453.	5.6	11

#	Article	IF	CITATIONS
163	Rapid analysis of Callicarpa L. using direct spray ionization mass spectrometry. Journal of Pharmaceutical and Biomedical Analysis, 2016, 124, 93-103.	2.8	15
164	Quantifying the Distribution of the Stoichiometric Composition of Anticancer Peptide Lycosin-I on the Lipid Membrane with Single Molecule Spectroscopy. Journal of Physical Chemistry B, 2016, 120, 3081-3088.	2.6	11
165	Carbon: Carbonâ€Based Sorbents with Threeâ€Dimensional Architectures for Water Remediation (Small) Tj ETQ	q110784 10.0784	4314 rgBT /O
166	Reduced Graphene Oxideâ€Wrapped MoO <sub>3</sub> Composites Prepared by Using Metal–Organic Frameworks as Precursor for Allâ€Solidâ€State Flexible Supercapacitors. Advanced Materials, 2015, 27, 4695-4701.	21.0	388
167	An iTRAQ-Based Proteomics Approach to Clarify the Molecular Physiology of Somatic Embryo Development in Prince Rupprecht's Larch (Larix principis-rupprechtii Mayr). PLoS ONE, 2015, 10, e0119987.	2.5	20
168	NaF-mediated controlled-synthesis of multicolor Na <sub>x</sub> ScF <sub>3+x</sub> :Yb/Er upconversion nanocrystals. Nanoscale, 2015, 7, 4048-4054.	5.6	33
169	AuAg Nanosheets Assembled from Ultrathin AuAg Nanowires. Journal of the American Chemical Society, 2015, 137, 1444-1447.	13.7	68
170	Geology and geochemistry of the Baijiantan–Baikouquan ophiolitic mélanges: implications for geological evolution of west Junggar, Xinjiang, NW China. Geological Magazine, 2015, 152, 41-69.	1.5	78
171	Facile synthesis of Cu <sub>2</sub> O nanocages and gas sensing performance towards gasoline. RSC Advances, 2015, 5, 54433-54438.	3.6	16
172	Sensors: DNA-Templated Silver Nanoclusters for Multiplexed Fluorescent DNA Detection (Small) Tj ETQq0 0 0 rgl	3T /Overlo 10.0	ck 10 Tf 50 3
173	Controlled Synthesis of Uniform Na <sub><i>x</i></sub> ScF <sub>3+<i>x</i></sub> Nanopolyhedrons, Nanoplates, Nanorods, and Nanospheres Using Solvents. Crystal Growth and Design, 2015, 15, 2988-2993.	3.0	18
174	Carbonâ€Based Sorbents with Threeâ€Dimensional Architectures for Water Remediation. Small, 2015, 11, 3319-3336.	10.0	166
175	Two-dimensional molybdenum disulphide nanosheet-covered metal nanoparticle array as a floating gate in multi-functional flash memories. Nanoscale, 2015, 7, 17496-17503.	5.6	28
176	Synthesis of high-quality lanthanide oxybromides nanocrystals with single-source precursor for promising applications in cancer cells imaging. Applied Materials Today, 2015, 1, 20-26.	4.3	20
177	Liquidâ€Phase Epitaxial Growth of Twoâ€Dimensional Semiconductor Heteroâ€nanostructures. Angewandte Chemie - International Edition, 2015, 54, 1841-1845.	13.8	88
178	DNAâ€Templated Silver Nanoclusters for Multiplexed Fluorescent DNA Detection. Small, 2015, 11, 1385-1389.	10.0	106
179	Singleâ€Layer Transition Metal Dichalcogenide Nanosheetâ€Based Nanosensors for Rapid, Sensitive, and Multiplexed Detection of DNA. Advanced Materials, 2015, 27, 935-939.	21.0	322
180	Oneâ€pot Synthesis of CdS Nanocrystals Hybridized with Single‣ayer Transitionâ€Metal Dichalcogenide Nanosheets for Efficient Photocatalytic Hydrogen Evolution. Angewandte Chemie - International Edition, 2015, 54, 1210-1214.	13.8	584

#	Article	IF	CITATIONS
181	Phosphineâ€Free, Lowâ€Temperature Synthesis of Tetrapodâ€Shaped CdS and Its Hybrid with Au Nanoparticles. Small, 2014, 10, 4727-4734.	10.0	20
182	TaS2 nanosheet-based room-temperature dosage meter for nitric oxide. APL Materials, 2014, 2, .	5.1	16
183	Analysis of Cigarette Smoke by Headspace Solid Phase Microextraction Gas Chromatography–Mass Spectrometry. Analytical Letters, 2014, 47, 1995-2002.	1.8	2
184	GC–MS Investigation of the Transfer Behavior of Alkalescent Flavors in Moderate/Low-Tar Cigarettes. Chromatographia, 2014, 77, 171-178.	1.3	1
185	Au Nanoparticleâ€Modified MoS <sub>2</sub> Nanosheetâ€Based Photoelectrochemical Cells for Water Splitting. Small, 2014, 10, 3537-3543.	10.0	265
186	MoS2 nanoflower-decorated reduced graphene oxide paper for high-performance hydrogen evolution reaction. Nanoscale, 2014, 6, 5624.	5.6	320
187	CdS: Phosphineâ€Free, Lowâ€Temperature Synthesis of Tetrapodâ€Shaped CdS and Its Hybrid with Au Nanoparticles (Small 22/2014). Small, 2014, 10, 4726-4726.	10.0	1
188	Coating Two-Dimensional Nanomaterials with Metal–Organic Frameworks. ACS Nano, 2014, 8, 8695-8701.	14.6	168
189	Single-crystalline Bi <sub>2</sub> Fe <sub>4</sub> O <sub>9</sub> synthesized by low-temperature co-precipitation: performance as photo- and Fenton catalysts. RSC Advances, 2014, 4, 27820-27829.	3.6	51
190	Water Splitting: Au Nanoparticle-Modified MoS2Nanosheet-Based Photoelectrochemical Cells for Water Splitting (Small 17/2014). Small, 2014, 10, 3536-3536.	10.0	2
191	A fluorometric biosensor based on H2O2-sensitive nanoclusters for the detection of acetylcholine. Biosensors and Bioelectronics, 2014, 59, 289-292.	10.1	38
192	Preparation of fine-grained α-alumina powder from seeded boehmite. Journal of Nanoparticle Research, 2013, 15, 1.	1.9	8
193	Carbon Fiber Aerogel Made from Raw Cotton: A Novel, Efficient and Recyclable Sorbent for Oils and Organic Solvents. Advanced Materials, 2013, 25, 5916-5921.	21.0	600
194	Surfactant assisted Ce–Fe mixed oxide decorated multiwalled carbon nanotubes and their arsenic adsorption performance. Journal of Materials Chemistry A, 2013, 1, 11355.	10.3	151
195	Electronic Effect Directed Au(I)-Catalyzed Cyclic C2–H Bond Functionalization of 3-Allenylindoles. Organic Letters, 2012, 14, 3616-3619.	4.6	63
196	Additive-assisted synthesis of boride, carbide, and nitride micro/nanocrystals. Journal of Solid State Chemistry, 2012, 194, 219-224.	2.9	24
197	Application of 1-Alkyl-3-methylimidazolium-Based Ionic Liquids as Background Electrolytes in Nonaqueous Capillary Electrophoresis for the Analysis of Coptidis Alkaloids. Analytical Letters, 2012, 45, 460-472.	1.8	4
198	Highly stable magnetic multiwalled carbon nanotube composites for solid-phase extraction of linear alkylbenzene sulfonates in environmental water samples prior to high-performance liquid chromatography analysis. Analyst, The, 2012, 137, 1232.	3.5	39

#	Article	IF	CITATIONS
199	The effects of functional polysiloxane resins on the color gamut and color yield of dyed polyester. Color Research and Application, 2012, 37, 72-75.	1.6	2
200	Fabrication of hollow cubic Ag microboxes with net-like nanofiber structures and their surface plasmon resonance. CrystEngComm, 2011, 13, 204-211.	2.6	7
201	In vitro evaluation of cytotoxicity and oxidative stress induced by multiwalled carbon nanotubes in murine RAW 264.7 macrophages and human A549 lung cells. Biomedical and Environmental Sciences, 2011, 24, 593-601.	0.2	38
202	Size-Controlled and Size-Designed Synthesis of Nano/Submicrometer Ag Particles. Crystal Growth and Design, 2010, 10, 3378-3386.	3.0	79
203	Optimal control of stepper motor stability program. , 2010, , .		2
204	Transmembrane Delivery of the Cell-Penetrating Peptide Conjugated Semiconductor Quantum Dots. Langmuir, 2008, 24, 11866-11871.	3.5	92
205	Chitosan nanoparticles for loading of toothpaste actives and adhesion on tooth analogs. Journal of Applied Polymer Science, 2007, 106, 4248-4256.	2.6	49
206	Defect-Rich, Candied Haws-Shaped AuPtNi Alloy Nanostructures for Highly Efficient Electrocatalysis. CCS Chemistry, 0, , 24-30.	7.8	0